

Multiple Access in the Delay-Doppler Domain using OTFS modulation

G. D. Surabhi, Rose Mary Augustine, and A. Chockalingam
Department of ECE, Indian Institute of Science, Bangalore 560012

Abstract—Orthogonal time frequency space (OTFS) modulation is a recent modulation scheme designed in the delay-Doppler domain. It has been shown to achieve superior performance compared to conventional multicarrier modulation schemes designed in the time-frequency domain. In this paper, we consider OTFS based multiple access (OTFS-MA), where delay-Doppler bins serve as the resource blocks for multiple access. Different delay-Doppler resource blocks (DDRBs) in the delay-Doppler grid are allocated to different users for multiple access. We consider three different DDRB allocation schemes. While Scheme 1 multiplexes the users along the delay axis, Scheme 2 multiplexes them along the Doppler axis. In both these schemes, each user's signal spans the entire time-frequency plane. Scheme 3 allocates the DDRBs in such a way that each user's signal is limited to span only over a subset of the time-frequency plane. We study the performance of OTFS-MA in high mobility environments on the uplink and compare it with those of OFDMA and SC-FDMA. Our results show that OTFS-MA (with maximum-likelihood detection in small dimension systems and with a message passing based detection in large dimension systems) achieves better performance compared to OFDMA and SC-FDMA. We also present the performance of a multiuser channel estimation scheme using pilot symbols placed in the delay-Doppler grid.

I. INTRODUCTION

Next generation wireless systems are envisioned to support high speed communications with energy efficiency and high reliability in various wireless environments. Enabling high speed and reliable communication in high mobility scenarios, which arise in environments such as high-speed trains, vehicle-to-vehicle, and vehicle-to-infrastructure communications, requires techniques which are specially suited for the dynamic nature of wireless channels. The wireless channels in such scenarios are rapidly time varying and hence doubly dispersive in nature, with the multipath effects causing time dispersion and Doppler shifts causing frequency dispersion [1]. Conventional multicarrier modulation techniques are primarily designed to combat the multipath effects that cause inter-symbol interference (ISI) [2]. However, high mobility or the use of high frequency carriers (e.g., mmWave frequencies) in low to medium mobility environments results in Doppler shift causing inter-carrier interference (ICI), which degrades the performance of conventional multicarrier modulation schemes.

Orthogonal time frequency space modulation (OTFS) is a new modulation technique suited for doubly dispersive wireless channels. OTFS was first introduced in [3], where

it was shown to outperform conventional multicarrier modulation schemes such as OFDM in channels with high Doppler spreads. The robustness of OTFS modulation in high mobility environments (e.g., vehicle speed as high as 500 km/h) and mmWave communication environments has been demonstrated in [3]-[6]. The basic idea behind OTFS modulation can be briefly explained as follows. OTFS is a 2-dimensional (2D) modulation technique which uses the delay-Doppler domain for multiplexing information symbols. This is in contrast to conventional multicarrier modulation schemes which multiplex symbols in the time-frequency domain. OTFS modulation uses a series of 2D transformations by which the rapidly time varying channel is converted into a slowly varying channel in the delay-Doppler domain. The slow variability of the delay-Doppler channels reduces the overhead of frequent channel estimation in channels with small coherence time. Also, these transformations are such that all the information symbols are coupled to the channel in the delay-Doppler domain in the same fashion. This greatly simplifies the equalizer design in rapidly time varying channels. Another attractive feature of OTFS is that it could be architected with pre- and post processing operations over any existing multicarrier system.

Recognizing the superior performance and implementation simplicity of OTFS, several works studying various aspects of OTFS have emerged recently [7]-[17]. A linear vector channel model for OTFS has been derived and a low-complexity message passing based OTFS signal detection scheme has been proposed in [9]. Another low-complexity OTFS signal detection scheme based on Markov chain Monte Carlo technique has been proposed in [10]. Low-complexity implementation of OTFS over conventional OFDM systems has been reported in [7],[8]. OTFS modulation in MIMO communication settings (MIMO-OTFS) with a focus on MIMO-OTFS signal detection and channel estimation has been reported in [11]. A diversity order analysis for OTFS has been presented in [12], where it has been shown that the asymptotic diversity order of OTFS (as $\text{SNR} \rightarrow \infty$) is one, and that, in the finite SNR regime, potential for a higher diversity slope is witnessed before the diversity one regime takes over. Space-time coding to achieve full spatial and delay-Doppler diversity in MIMO-OTFS systems is proposed in [13]. In [14], the performance of OTFS with practical pulse shaping has been considered. A framework that relates the generalized frequency division multiplexing (GFDM) and OTFS has been formulated in [15] and a bit error performance comparison showed that OTFS performs better than GFDM.

In this paper, we consider OTFS modulation for multiuser

This work was supported in part by the J. C. Bose National Fellowship, Department of Science and Technology, Government of India, and the Intel India Faculty Excellence Program.

communication on the uplink, where users are multiplexed on the delay-Doppler grid which is designed by considering the maximum delay and Doppler spreads of the multiuser channel. In this multiple access system, called as OTFS-MA (OTFS multiple access), bins in the delay-Doppler grid serve as the resource blocks. These resource blocks are called the DDRBs (delay-Doppler resource blocks). Different DDRBs are allocated to different users for multiple access. We consider three different DDRB allocation schemes. While Scheme 1 multiplexes the users along the delay axis, Scheme 2 multiplexes them along the Doppler axis. In both these schemes, each user's signal spans the entire time-frequency plane. Scheme 3 allocates the DDRBs in such a way that each user's signal is limited to span over only a subset of the time-frequency plane. All these three schemes have been suggested in [4]. The sum rate of Scheme 3 has been analyzed in [16]. Here, we study the bit error performance of OTFS-MA with the above allocation schemes in high mobility environments on the uplink and compare it with those of other popular multiple access schemes such as OFDMA and SC-FDMA. Our results show that OTFS-MA (with maximum-likelihood detection in small dimension systems and with a message passing based detection in large dimension systems) achieves better performance compared to OFDMA and SC-FDMA. We also present the performance of a multiuser channel estimation scheme using pilot symbols placed in the delay-Doppler grid.

The rest of this paper is organized as follows. In Sec. II, the OTFS-MA system model and the DDRB allocation schemes considered are presented. In Sec. III, the performance of OTFS-MA under the considered allocation schemes are compared. A comparison between OTFS-MA, OFDMA, and SC-FDMA with ML detection is also presented. In Sec. IV, a message passing based detection and its performance are presented. A channel estimation technique for OTFS-MA and its performance are presented in Sec. V. Conclusions are presented in Sec. VI.

II. OTFS-MA SYSTEM MODEL

A. Uplink OTFS-MA system model

Consider an OTFS-MA system with K_u uplink users communicating with a base station (BS) as shown in Fig. 1. Each user employs OTFS modulation for signaling on the uplink. Each user is equipped with a single antenna transmitter and the BS is equipped with a single antenna receiver. In OTFS, information symbols are multiplexed in the delay-Doppler domain, i.e., the information symbols are multiplexed on an $N \times M$ delay-Doppler grid which is denoted by Γ , and is given by

$$\Gamma = \{(\frac{k}{NT}, \frac{l}{M\Delta f}), k = 0, 1, \dots, N-1, l = 0, 1, \dots, M-1\}. \quad (1)$$

Here, $1/NT$ and $1/M\Delta f$ represent the quantization steps of the Doppler shift and the delay, respectively, so that N and M denote the number of Doppler and delay bins, respectively. Let τ_{\max} and ν_{\max} denote the maximum delay and Doppler spread of the multiuser channel, respectively. Then, Δf must

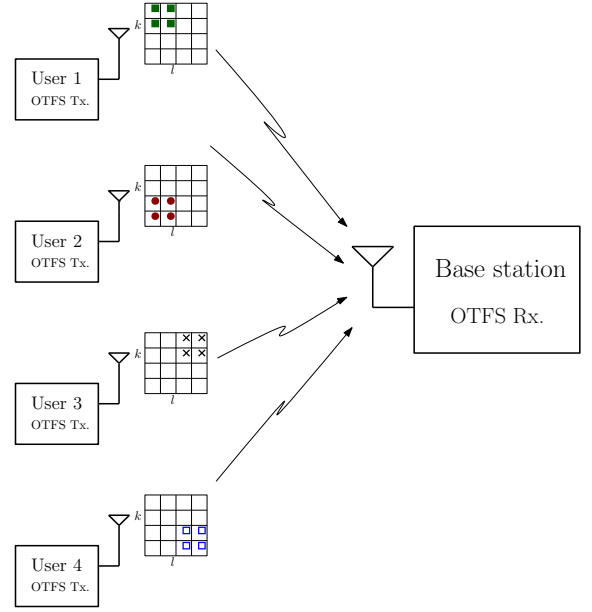


Fig. 1: OTFS multiple access (OTFS-MA) on the uplink.

be such that $\nu_{\max} < \Delta f < 1/\tau_{\max}$. We refer to a bin on the delay-Doppler grid Γ in (1) as a delay-Doppler resource block (DDRb). Let $x_u[k, l]$, $k = 0, 1, \dots, N-1$, $l = 0, 1, \dots, M-1$, and $u = 0, 1, \dots, K_u-1$ denote the information symbol from a modulation alphabet \mathbb{A} (e.g., QAM/PSK) transmitted by the u th user on the (k, l) th DDRb.

The information symbols of the u th user, i.e., $x_u[k, l]$ s, in the delay-Doppler domain are mapped to the TF domain using the inverse symplectic finite Fourier transform (ISFFT) and windowing. Assuming rectangular windowing, the modulated TF signal corresponding to the u th user is given by

$$X_u[n, m] = \frac{1}{\sqrt{MN}} \sum_{k=0}^{N-1} \sum_{l=0}^{M-1} x_u[k, l] e^{j2\pi(\frac{nk}{N} - \frac{ml}{M})}. \quad (2)$$

The TF signal so obtained is converted into a time domain signal for transmission using Heisenberg transform with a transmit pulse denoted by $g_{tx}(t)$. The transmitted time domain signal of the u th user therefore is given by

$$x_u(t) = \sum_{n=0}^{N-1} \sum_{m=0}^{M-1} X_u[n, m] g_{tx}(t - nT) e^{j2\pi m \Delta f (t - nT)}. \quad (3)$$

The transmitted signal $x_u(t)$ passes through the channel whose complex baseband channel response in the delay-Doppler domain is denoted by $h_u(\tau, \nu)$. The received time domain signal $y(t)$ at the BS is given by

$$y(t) = \sum_{u=0}^{K_u-1} \int_{\nu} \int_{\tau} h_u(\tau, \nu) x_u(t - \tau) e^{j2\pi \nu (t - \tau)} d\tau d\nu + v(t), \quad (4)$$

where $h_u(\tau, \nu)$ is the delay-Doppler channel between the u th user and the BS and $v(t)$ denotes the additive white Gaussian noise at the BS receiver. The received signal at the BS is

matched filtered with a receive pulse $g_{rx}(t)$, yielding the cross-ambiguity function denoted by $A_{g_{rx},y}(t, f)$ and given by

$$A_{g_{rx},y}(t, f) = \int g_{rx}^*(t' - t)y(t')e^{-j2\pi f(t' - t)}dt'. \quad (5)$$

The pulses $g_{tx}(t)$ and $g_{rx}(t)$ are chosen such that the biorthogonality condition is satisfied, i.e., $A_{g_{rx},g_{tx}}(t, f)|_{nT, m\Delta f} = \delta(m)\delta(n)$. Sampling $A_{g_{rx},y}(t, f)$ at $t = nT$ and $f = m\Delta f$ yields the matched filter output, given by

$$Y[n, m] = A_{g_{rx},y}(t, f)|_{t=nT, f=m\Delta f}. \quad (6)$$

Finally, $Y[n, m]$ is converted from TF domain back to delay-Doppler domain to obtain $y[k, l]$ as

$$y[k, l] = \frac{1}{\sqrt{MN}} \sum_{k=0}^{N-1} \sum_{l=0}^{M-1} Y[n, m] e^{-j2\pi(\frac{nk}{N} - \frac{ml}{M})}. \quad (7)$$

If $h_u(\tau, \nu)$ has finite support bounded by $(\tau_{\max}, \nu_{\max})$ and if $A_{g_{rx},g_{tx}}(t, f) = 0$ for $t \in (nT - \tau_{\max}, nT + \tau_{\max})$, $f \in (m\Delta f - \nu_{\max}, m\Delta f + \nu_{\max})$, $\forall (n, m) \neq (0, 0)$, the end-to-end input-output relation for the considered uplink OTFS-MA system can be written as

$$y[k', l'] = \frac{1}{MN} \sum_{u=0}^{K_u-1} \sum_{k=0}^{N-1} \sum_{l=0}^{M-1} x_u[k, l] \tilde{h}_u[(k' - k)_N, (l' - l)_M] + v[k', l'], \quad (8)$$

where $(\cdot)_N$ denotes modulo- N operation, $v[k, l]$ denotes the additive white Gaussian noise, and $\tilde{h}_u(k, l)$ is the sampled version of the impulse response function $\tilde{h}_u(\nu, \tau)$, which is the circular convolution of $h_u(\tau, \nu)$ with the window function in the delay-Doppler domain, at $\nu = \frac{k}{NT}$ and $\tau = \frac{l}{M\Delta f}$ [3].

Consider that the channel between the u th user and the BS, i.e., $h_u(\tau, \nu)$, has P_u paths, where $h_{u,i}$, $\tau_{u,i}$, $\nu_{u,i}$ denote the channel gain, delay, and Doppler shift, respectively, associated with the i th path of the u th user. The u th user's channel in the delay-Doppler domain is then given by

$$h_u(\tau, \nu) = \sum_{i=1}^{P_u} h_{u,i} \delta(\tau - \tau_{u,i}) \delta(\nu - \nu_{u,i}), \quad (9)$$

where $h_{u,i}$ s are assumed to be i.i.d. Let $\tau_{u,i} \triangleq \frac{\alpha_{u,i}}{M\Delta f}$ and $\nu_{u,i} \triangleq \frac{\beta_{u,i} + b_{u,i}}{NT}$, where $\alpha_{u,i}$, $\beta_{u,i}$ are integers and $-\frac{1}{2} < b_{u,i} \leq \frac{1}{2}$ is the fractional Doppler corresponding to $\nu_{u,i}$. Fractional delays are not considered since the sampling time (delay resolution $1/M\Delta f$) is typically small in wideband systems and hence it can be approximated to the nearest sampling point [19]. With this, the input-output relation is given by

$$y[k, l] = \sum_{u=0}^{K_u-1} \sum_{i=1}^{P_u} \sum_{q'=0}^{N-1} \left(\frac{e^{-j2\pi(-q' - b_{u,i})} - 1}{Ne^{-j\frac{2\pi}{N}(-q' - b_{u,i})} - N} \right) h_{u,i} \cdot e^{-j2\pi\tau_{u,i}\nu_{u,i}} x_u[(k - \beta_{u,i} + q')_N, (l - \alpha_{u,i})_M] + v[k, l]. \quad (10)$$

The 2D circular convolution of symbols transmitted by each user with the corresponding channel in (8) can be written in

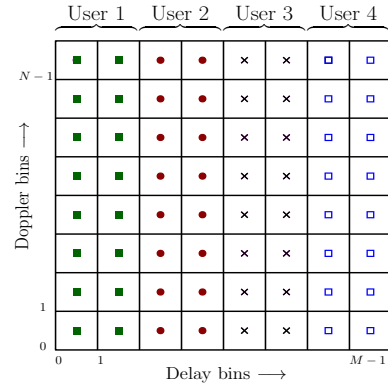


Fig. 2: DDRB allocation in an $N \times M$ delay-Doppler grid in Scheme 1.

a vectorized form as in the case of single user setting [9]. Denoting the OTFS symbol vector transmitted by u th user by $\mathbf{x}_u \in \mathbb{C}^{MN \times 1}$ ($\mathbf{x}_u[k + Nl] = x_u[k, l]$) and the channel matrix of u th user by $\mathbf{H}_u \in \mathbb{C}^{MN \times MN}$, the input-output relation in multiuser OTFS can be written as

$$\mathbf{y} = \sum_{u=0}^{K_u-1} \mathbf{H}_u \mathbf{x}_u + \mathbf{v},$$

$$= [\mathbf{H}_1 \mathbf{H}_2 \cdots \mathbf{H}_{K_u}] \begin{bmatrix} \mathbf{x}_1 \\ \mathbf{x}_2 \\ \vdots \\ \mathbf{x}_{K_u} \end{bmatrix} + \mathbf{v}, \quad (11)$$

where $\mathbf{y} \in \mathbb{C}^{MN \times 1}$ is the received vector at the BS, and \mathbf{v} is the additive white Gaussian noise vector with $\mathbf{v}_{k+Nl} = v[k, l]$.

B. DDRB allocation schemes

In this subsection, we present three different schemes for allocation of DDRBs to users in an uplink OTFS-MA system.

1) *Scheme 1 (Multiplexing users along the delay axis):* In this scheme, disjoint and contiguous bins along the delay axis are allocated to each user such that each user gets M/K_u columns of the delay-Doppler grid for transmission (see Fig. 2). The delay-Doppler grid of the u th user will have

$$x_u[k, l] = \begin{cases} a \in \mathbb{A} & \text{if } k \in \{0, 1 \cdots N-1\} \& \\ & l \in \{u \frac{M}{K_u}, \cdots (u+1) \frac{M}{K_u} - 1\} \\ 0 & \text{otherwise.} \end{cases} \quad (12)$$

Figure 2 shows an example of Scheme 1 allocation, where an $N \times M = 8 \times 8$ delay-Doppler grid gets allocated to four users. Note that, although the users transmit on non-overlapping DDRBs, the symbols transmitted by each user experience multiuser interference (MUI) due to the 2D circular convolution operation in (8). The amount of MUI experienced depends on the delay spread of the channels. Hence, the received signal at the BS has to be jointly decoded. A way to receive MUI free signal at the BS using Scheme 1 is to use a set of DDRBs as guard bands in the delay domain, based on the delay spread of the adjacent users' channels [18]. However, this reduces the spectral efficiency of the overall

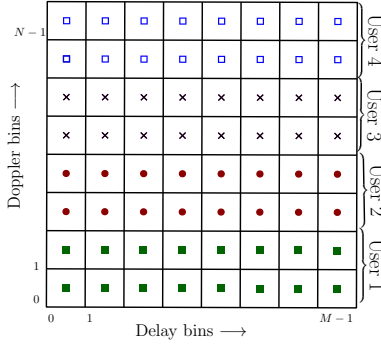


Fig. 3: DDRB allocation in an $N \times M$ delay-Doppler grid in Scheme 2.

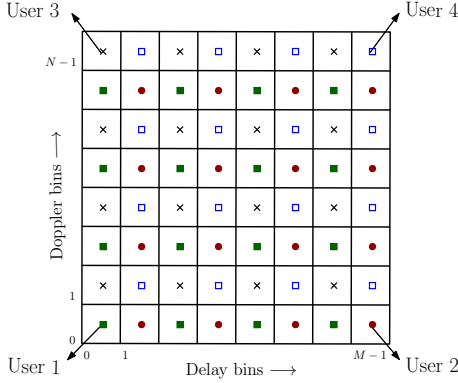


Fig. 4: DDRB allocation in an $N \times M$ delay-Doppler grid in Scheme 3 [16].

system, especially in the channels with large delay spreads which require large guard bands for MUI-free reception.

2) *Scheme 2 (Multiplexing users along the Doppler axis):* In this scheme, non-overlapping and contiguous DDRBs along the Doppler axis are allocated to each user such that each user gets N/K_u rows of the delay-Doppler grid for transmission (see Fig. 3). The delay-Doppler grid of the u th user will have

$$x_u[k, l] = \begin{cases} a \in \mathbb{A} & \text{if } k \in \{u \frac{N}{K_u}, \dots, (u+1) \frac{N}{K_u} - 1\} \text{ \& } \\ & l \in \{0, 1, \dots, M-1\} \\ 0 & \text{otherwise.} \end{cases} \quad (13)$$

Figure 3 shows an example of Scheme 2 allocation, where an $N \times M = 8 \times 8$ delay-Doppler grid gets allocated to four users. In Scheme 2 also, the 2D circular convolution operation in (8) results in the symbols transmitted by each user to experience MUI, requiring the BS to jointly decode the symbols corresponding to all the users. Allowing guard bands along the Doppler domain can result in MUI-free reception at the BS [18]. However, for channels with high Doppler spread, this may result in reduced spectral efficiency of the system.

3) *Scheme 3 (Allocation scheme in [16]):* In Schemes 1 and 2, each user's signal spans the entire time-frequency plane. In Scheme 3 [16], the allocation of DDRBs is done in such a way that each user's signal can be restricted to span only over a subset of the time-frequency plane. The allocation is such that MN/K_u symbols corresponding to a given user are placed

at equal intervals in the delay as well as Doppler domains (see Fig. 4). These intervals are determined by two parameters denoted by g_1 and g_2 such that $K_u = g_1 g_2$, with $M = \kappa_1 g_1$ and $N = \kappa_2 g_2$, where $\kappa_1, \kappa_2 \in \mathbb{Z}_+$. The allocation is such that the delay-Doppler grid corresponding to the u th user will have

$$x_u[k, l] = \begin{cases} a \in \mathbb{A} & \text{if } k = \lfloor u/g_1 \rfloor + g_2 p \text{ \& } \\ & l = (u)_{g_1} + g_1 q \\ 0 & \text{otherwise.} \end{cases} \quad (14)$$

where $p \in \{0, 1, \dots, N/g_2 - 1\}$ and $q \in \{0, 1, \dots, M/g_1 - 1\}$. This scheme results in a periodic interleaving of symbols from each user as shown in Fig. 4 for a system with $M = N = 8$, $K_u = 4$, and $g_1 = g_2 = 2$. It has been shown in [16] that, with this allocation, the time-frequency symbols $X_u[n, m]$ corresponding to u th user can be restricted to a region $[(NT/g_2)(u)_{g_2}, (NT/g_2)((u)_{g_2} + 1)]$ in time and $[(M/g_1)\lfloor u/g_2 \rfloor \Delta f, (M/g_1)(\lfloor u/g_2 \rfloor + 1)\Delta f]$ in frequency. These regions are non-overlapping in the TF plane, and hence it enables the BS to separate out the received TF signal of each user. At the BS, the TF signal of u th user, denoted by $Y_u[n, m]$, is transformed back to the delay-Doppler domain through SFFT as [16]

$$y_u[k', l'] = \frac{1}{\sqrt{MN}} \sum_{n=0}^{N/g_2-1} \sum_{m=0}^{M/g_1-1} Y_u[n, m] e^{-j2\pi(\frac{nk'}{N/g_2} - \frac{ml'}{M/g_1})}. \quad (15)$$

The SFFT in (15) results in the u th user's signal in delay-Doppler domain $y_u[k', l']$, $k' = 0, 1, \dots, N/g_2 - 1$, $l' = 0, 1, \dots, M/g_1 - 1$. Note that the SFFT computation in (15) is over the region in TF domain to which the u th user's signal is restricted to. This is unlike the SFFT computation in (7), which involved computing SFFT over the entire TF plane. This difference in SFFT computation results in a slightly different input-output relation for Scheme 3 compared to those of Schemes 1 and 2. The input-output relation for Scheme 3 has been derived in [16] and is given by

$$y_u[k', l'] = \sum_{k=0}^{N/g_2-1} \sum_{l=0}^{M/g_1-1} \tilde{x}_u[k, l] \hat{h}_u[(k' - k)_{N/g_2}, (l' - l)_{M/g_1}] + v_q[k', l'], \quad (16)$$

where $\tilde{x}_u[p, q] \triangleq x_u(k = \lfloor u/g_1 \rfloor + g_2 p, l = (u)_{g_1} + g_1 q)$ and $v_q[k', l'] \sim \mathcal{CN}(0, 1/(g_1 g_2))$, and

$$\begin{aligned} \hat{h}_u[r, s] &= \sum_{i=1}^{P_u} [h_{u,i} e^{-j2\pi(\nu_{u,i} \tau_{u,i} + \frac{\tau_{u,i}}{T} \lfloor \frac{u}{g_2} \rfloor - \frac{\nu_{u,i}}{\Delta f} \frac{N}{g_2} (u)_{g_2})} \\ &\quad \mathcal{F}_{u,i}[s] \mathcal{G}_{u,i}[r]], \\ \mathcal{F}_{u,i}[s] &= \frac{1}{M} \sum_{m=0}^{M/g_1-1} e^{-j2\pi m \left(\frac{(u)_{g_1}}{M} - \frac{s}{M/g_1} + \frac{\tau_{u,i}}{T} \right)}, \\ \mathcal{G}_{u,i}[r] &= \frac{1}{N} \sum_{n=0}^{N/g_2-1} e^{j2\pi n \left(\frac{\lfloor u/g_1 \rfloor}{N} - \frac{r}{N/g_2} + \frac{\nu_{u,i}}{\Delta f} \right)}. \end{aligned} \quad (17)$$

The 2D convolution in (16) can be vectorized as

$$\mathbf{y}_u = \hat{\mathbf{H}}_u \tilde{\mathbf{x}}_u + \tilde{\mathbf{v}}_u, \quad (18)$$

where $\tilde{\mathbf{x}}_u \in \mathbb{C}^{MN/K_u \times 1}$ and $\hat{\mathbf{H}}_u \in \mathbb{C}^{MN/K_u \times MN/K_u}$. Since users' signals at the BS in this scheme are separable in the TF plane, the TF signal corresponding to each user can be individually mapped to the delay-Doppler plane for detection. This leads to reduced detection complexity at the BS.

III. ML DETECTION PERFORMANCE RESULTS

In this section, we present the bit error rate (BER) performance of uplink OTFS-MA under ML detection. We compare the performance of the DDRB allocation schemes presented in Sec. II-B. We also compare the BER performance of OTFS-MA with those of OFDMA and SC-FDMA.

Performance of DDRB allocation Schemes 1,2,3: Figure 5 shows the BER performance of uplink OTFS-MA with the different DDRB allocation schemes discussed in Sec. II-B. A delay-Doppler grid with $M = N = 4$ is considered. The delay-Doppler bins in this grid are shared among $K_u = 2$ users. A carrier frequency of 4 GHz, subcarrier spacing of 15 kHz, and BPSK modulation are used. A four-tap delay-Doppler channel ($P_u = 4, \forall u$) with exponential power delay profile and Jakes Doppler spectrum [20] is considered for all the users. The Doppler shift corresponding to the i th tap of u th user is generated using $\nu_{u,i} = \nu_{\max} \cos(\theta_{u,i})$, where ν_{\max} is the maximum Doppler shift which is taken to be 1 kHz for all the users and $\theta_{u,i}$ is uniformly distributed over $[-\pi, \pi]$. From Fig. 5, we observe that the BER performance of OTFS-MA using the allocation Scheme 1 (in Sec. II-B1) and Scheme 2 (in Sec. II-B2) is nearly the same and is superior compared to that of Scheme 3 (in Sec. II-B3). This can be explained as follows. In Scheme 3, each user's symbols are allowed to spread only in a restricted and disjoint region in the time-frequency plane, whereas the symbols in Schemes 1 and 2 are allowed to spread over the entire TF plane. In Scheme 3, the restricted spreading of each user's signal in the TF plane when brought back to the delay-Doppler plane through a reduced point SFFT operation hurts the bit error performance. Whereas, in Schemes 1 and 2, the spreading of each user's signal over the entire TF plane and the full point SFFT operation to bring back this TF signal to the delay-Doppler plane followed by joint detection of all users' symbols result in improved performance compared to that of Scheme 3. An issue with the joint detection is its high complexity. We address this issue in Sec. IV where a low complexity joint detection scheme is proposed using message passing approach.

Effect of number of uplink users: In Fig. 6, we plot the BER performance of OTFS-MA with DDRB allocation Schemes 1, 2, and 3, for $K_u = 2, 4, 8$. All the other parameters are the same as those used in Fig. 5. From Fig. 6, it can be seen that Schemes 1 and 2 show nearly the same performance with increase in the number of uplink users due to joint detection. Also, Schemes 1 and 2 outperform Scheme 3. It can be seen that, unlike Schemes 1 and 2, the BER performance with Scheme 3 degrades with the increase in the number of uplink

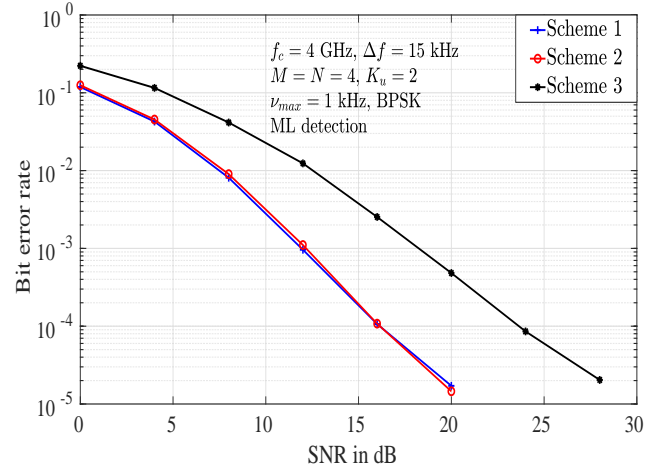


Fig. 5: BER performance of uplink OTFS-MA with different DDRB allocation schemes with $M = N = 4$, $K_u = 2$, and ML detection.

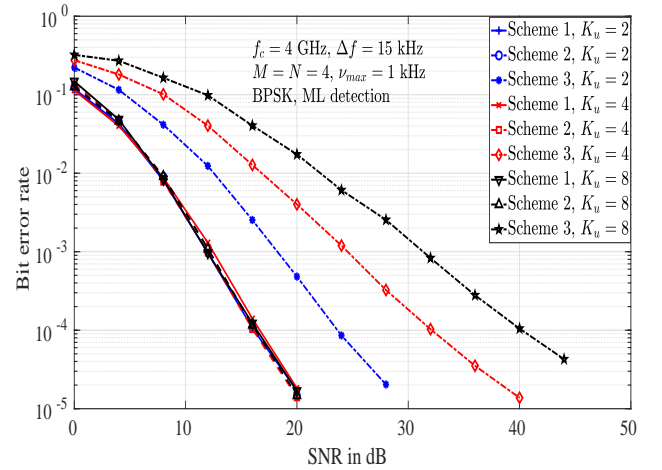


Fig. 6: BER performance of uplink OTFS-MA with different DDRB allocation schemes with $M = N = 4$, $K_u = 2, 4, 8$, and ML detection.

users. This can be explained as follows. As mentioned before, the transmitted TF signal of each user in Scheme 3 is restricted to a specific region in the TF plane. The size of this region in the TF plane over which the symbols are spread is inversely proportional to the number of users. Therefore, increase in the number of users for a given M and N reduces the spread in the TF plane for each user, which degrades the performance of the system.

Comparison between OTFS-MA, OFDMA, and SC-FDMA: Figure 7 shows a BER performance comparison between OTFS-MA with Scheme 1 allocation, OFDMA, and SC-FDMA. As before, a carrier frequency of 4 GHz, a subcarrier spacing of 15 kHz, exponential power delay profile, and Jakes Doppler spectrum are considered. For all the three systems, joint ML detection is used at the BS. The maximum Doppler considered is 1 kHz, which corresponds to a speed

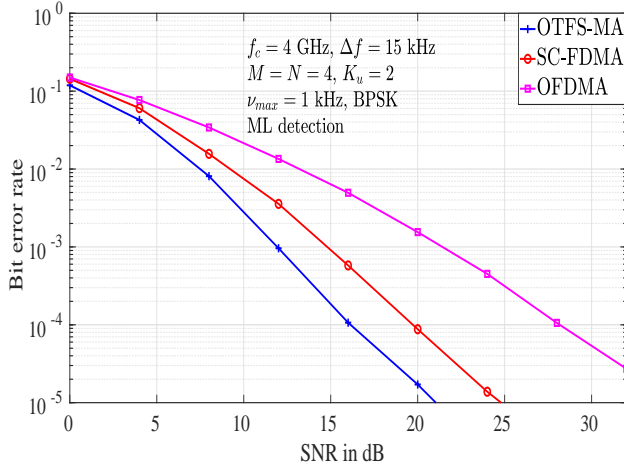


Fig. 7: BER performance comparison between OTFS-MA, OFDMA, and SC-FDMA with ML detection.

of 270 km/h at 4 GHz carrier frequency. The Doppler shift corresponding to the i th tap of u th user's channel is generated using $\nu_{u,i} = \nu_{\max} \cos(\theta_{u,i})$, where ν_{\max} is the maximum Doppler shift and $\theta_{u,i}$ is uniformly distributed over $[-\pi, \pi]$. From Fig. 7, it can be seen that the performance of OTFS-MA is superior compared to the performance of both OFDMA and SC-FDMA. For example, OTFS-MA achieves an SNR gain of about 4 dB and 12 dB compared to SC-FDMA and OFDMA, respectively, at a BER of 10^{-4} .

IV. MESSAGE PASSING DETECTION FOR OTFS-MA

Although ML detection is optimal, its complexity grows exponentially with M and N . In this section, we present a low complexity message passing based signal detection algorithm for OTFS-MA. Consider the OTFS-MA system model in (11). Let Ω denote the support (positions of non-zeros) of the OTFS-MA transmit signal vector $[\mathbf{x}_1^T \mathbf{x}_2^T \cdots \mathbf{x}_{K_u}^T]^T$. Then, the system in (11) can be alternatively written as

$$\mathbf{y} = \mathbf{H}\mathbf{x} + \mathbf{v}, \quad (19)$$

where $\mathbf{H} = [\mathbf{H}_1 \mathbf{H}_2 \cdots \mathbf{H}_{K_u}]_{\Omega}$ is the channel restricted to Ω and $\mathbf{x} = [\mathbf{x}_1^T \mathbf{x}_2^T \cdots \mathbf{x}_{K_u}^T]_{\Omega}^T$ is the non-zero part of the OTFS-MA transmit vector. Then, (19) can be modeled as a sparsely connected factor graph with NM variable nodes corresponding to \mathbf{x} and NM observation nodes corresponding to \mathbf{y} . Denoting the support of the s th row of \mathbf{H} by φ_s and the support of the r th column of \mathbf{H} by φ_r , each observation node y_s is connected to the set of variable nodes $\{x_t, t \in \varphi_s\}$, and each variable node x_r is connected to the set of observation nodes $\{y_t, t \in \varphi_r\}$. With this, the maximum a posteriori (MAP) detection rule for estimating the transmitted signal vector \mathbf{x} is given by

$$\hat{\mathbf{x}} = \underset{\mathbf{x} \in \mathbb{A}^{NM}}{\operatorname{argmax}} \Pr(\mathbf{x}|\mathbf{y}, \mathbf{H}). \quad (20)$$

The joint MAP detection in (20) has exponential complexity. Hence, we use symbol by symbol MAP rule for $0 \leq r \leq NM - 1$ for detection as follows:

$$\begin{aligned} \hat{x}_r &= \underset{a_j \in \mathbb{A}}{\operatorname{argmax}} \Pr(x_r = a_j | \mathbf{y}, \mathbf{H}) \\ &= \underset{a_j \in \mathbb{A}}{\operatorname{argmax}} \frac{1}{|\mathbb{A}|} \Pr(\mathbf{y} | x_r = a_j, \mathbf{H}) \\ &\approx \underset{a_j \in \mathbb{A}}{\operatorname{argmax}} \prod_{t \in \varphi_r} \Pr(y_t | x_r = a_j, \mathbf{H}). \end{aligned} \quad (21)$$

Since the transmitted symbols can be assumed to be equally likely and the components of \mathbf{y} can be assumed to be nearly independent for a given x_r , due to the sparsity in \mathbf{H} , (21) can be solved using a message passing (MP) based approach. The message that is passed from the variable node x_r , for each $r = \{0, 1, \dots, NM - 1\}$, to the observation node y_s for $s \in \varphi_r$, is the pmf denoted by $\mathbf{p}_{rs} = \{p_{rs}(a_j) | a_j \in \mathbb{A}\}$ of the symbols in the constellation \mathbb{A} . The steps involved in message passing detection can be described as follows:

- 1: **Inputs:** $\mathbf{y}, \mathbf{H}, n_{\max}$: maximum number of iterations.
- 2: **Initialization:** Iteration index $k = 0$, pmf $\mathbf{p}_{rs}^{(0)} = 1/|\mathbb{A}| \forall r \in \{0, 1, \dots, NM - 1\}$ and $s \in \varphi_r$.
- 3: **Messages from y_s to x_r :** The message passed from y_s to x_r is a Gaussian pdf which can be computed from

$$y_s = x_r H_{s,r} + \underbrace{\sum_{t \in \varphi_s, t \neq r} x_t H_{s,t}}_{I_{sr}} + v_s. \quad (22)$$

The interference plus noise term I_{sr} is approximated as a Gaussian r. v. with mean and variance given by

$$\begin{aligned} \mu_{sr}^{(k)} &= \mathbb{E}[I_{sr}] = \sum_{t \in \varphi_s, t \neq r} \sum_{j=1}^{|\mathbb{A}|} p_{ts}^{(k)}(a_j) a_j H_{s,t}, \\ (\sigma_{sr}^{(k)})^2 &= \operatorname{Var}[I_{sr}] \\ &= \sum_{t \in \varphi_s, t \neq r} \left(\sum_{j=1}^{|\mathbb{A}|} p_{ts}^{(k)}(a_j) |a_j|^2 |H_{s,t}|^2 - \left| \sum_{j=1}^{|\mathbb{A}|} p_{ts}^{(k)}(a_j) a_j H_{s,t} \right|^2 \right) \\ &\quad + \sigma^2. \end{aligned}$$

- 4: **Messages from x_r to y_s :** Message passed from variable nodes x_r to observation nodes y_s is the pmf vector $\mathbf{p}_{rs}^{(k+1)}$ with the entries given by

$$p_{rs}^{(k+1)} = \Delta p_{rs}^{(k)}(a_j) + (1 - \Delta) p_{rs}^{(k-1)}(a_j), \quad (23)$$

where $\Delta \in (0, 1]$ is the damping factor for improving convergence rate, and

$$p_{rs}^{(k)} \propto \prod_{t \in \varphi_r, t \neq s} \Pr(y_t | x_r = a_j, \mathbf{H}), \quad (24)$$

where

$$\Pr(y_t | x_r = a_j, \mathbf{H}) \propto \exp \left(\frac{-|y_t - \mu_{tr}^{(k)} - H_{t,r} a_j|^2}{\sigma_{t,r}^{2(k)}} \right).$$

- 5: **Stopping criterion:** Repeat steps 3 and 4 till $\max_{r,s,a_j} |p_{rs}^{(k+1)}(a_j) - p_{rs}^{(k)}(a_j)| < \epsilon$ (where ϵ is a small

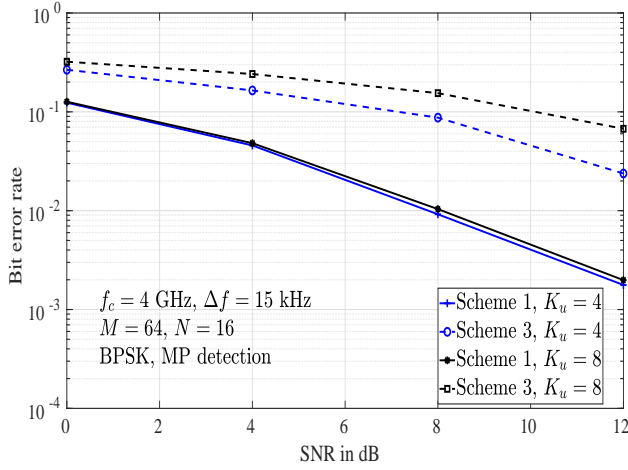


Fig. 8: BER performance of uplink OTFS-MA with DDRB allocation Schemes 1 and 3 with $K_u = 4, 8$ users, $M = 64$, $N = 16$, and MP detection.

value) or the maximum number of iterations, n_{max} , is reached.

6: **Output:** Output the detected symbol as

$$\hat{x}_r = \underset{a_j \in \mathbb{A}}{\operatorname{argmax}} p_r(a_j), \quad r \in 0, 1, 2, \dots, NM - 1, \quad (25)$$

where

$$p_r(a_j) = \prod_{t \in \varphi_r} \Pr(y_t | x_r = a_j, \mathbf{H}). \quad (26)$$

A. BER performance results with MP detection

Figure 8 shows the BER performance of OTFS-MA with DDRB allocation Schemes 1 and 3 using MP detection. All the systems considered use a carrier frequency of 4 GHz, a subcarrier spacing of 15 kHz, and BPSK modulation. For all the users, we have considered a 10-tap channel with exponential power delay profile and Jakes Doppler spectrum. The delay taps considered for each user's channel is $\tau_{u,i} = [0, 1.04, 2.08, 3.12, 4.16, 5.2, 6.25, 7.29, 8.33, 9.37] \mu s \forall u \in \{0, 1, \dots, K_u - 1\}$. The Doppler shift corresponding to the i th tap of u th user's channel is generated using $\nu_{u,i} = \nu_{\max} \cos(\theta_{u,i})$, where ν_{\max} is the maximum Doppler shift and $\theta_{u,i}$ is uniformly distributed over $[-\pi, \pi]$. The maximum Doppler shift considered is 1 kHz for all the users which corresponds to a velocity of 270 km/h. We have used a delay-Doppler grid with $M = 64$ and $N = 16$ and plotted the BER performance of Schemes 1 and 3 with $K_u = 4$ and 8, using the MP detection. From the Fig. 8, we observe that the performance of Scheme 1 is superior compared to that of Scheme 3. Also, the performance of Scheme 1 does not degrade with the increase in the number of uplink users, whereas the performance of Scheme 3 degrades with the increase in the number of users, as observed with ML detection in Sec. III.

Comparison between OTFS-MA, OFDMA, and SC-FDMA: Figure 9 shows the BER performance of OTFS-MA with

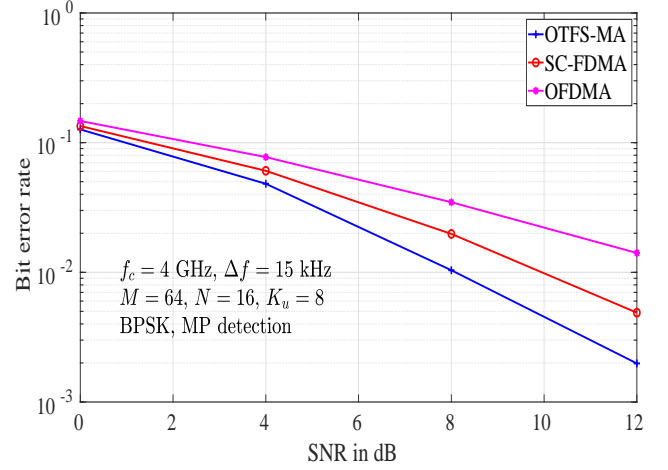


Fig. 9: BER performance comparison between OTFS-MA, OFDMA, and SC-FDMA with MP detection.

allocation Scheme 1, OFDMA, and SC-FDMA using message passing detection. OTFS-MA uses an $N \times M = 16 \times 64$ delay-Doppler grid which is allocated to $K_u = 8$ users. All the systems use 4 GHz carrier frequency and a subcarrier spacing of 15 kHz. The channel corresponding to each user is assumed to have ten taps ($P_u = 10, \forall u$) with an exponential power delay profile and Jakes Doppler spectrum. All the other simulation parameters considered are the same as those used in Fig. 8. From Fig. 9, it can be seen that OTFS-MA achieves superior performance compared to OFDMA and SC-FDMA, reiterating the results obtained with ML detection in Sec. III.

V. CHANNEL ESTIMATION IN OTFS-MA

In this section, we present a channel estimation technique for uplink OTFS-MA with DDRB allocation Schemes 1 and 2. This technique uses an impulse function ($\delta(k, l)$) in the delay-Doppler domain as the pilot. The pilot corresponding to each user is placed in the delay-Doppler grid such that they can be received without interference at the BS. The pilot corresponding to the u th user is an impulse denoted by $\delta(k_u^p, l_u^p)$, such that the point (k_u^p, l_u^p) is a DDRB allocated to the u th user. Each user's pilot has a space reserved around it in the delay-Doppler plane to account for the maximum delay and Doppler spread of the channel. Since the transmitted pilots are impulse functions, they are spread by the channel to the extent of the support of each user's channel in the delay-Doppler domain. Hence, if the pilots are placed sufficiently far apart in the delay-Doppler plane, they can be received at the BS without interference. For the placement of pilots of different users, we take into account fractional Dopplers in the channels as in (10). From (10), it can be seen that due to the fractional Doppler values, the channel spreads completely along the Doppler domain [17]. Hence, the pilot corresponding to the u th user, denoted by $x_u^p[k, l]$ is placed such that

$$x_u^p[k, l] = \begin{cases} 1 & \text{if } k = k_u^p, l = l_u^p, \\ 0 & \text{otherwise.} \end{cases} \quad (27)$$

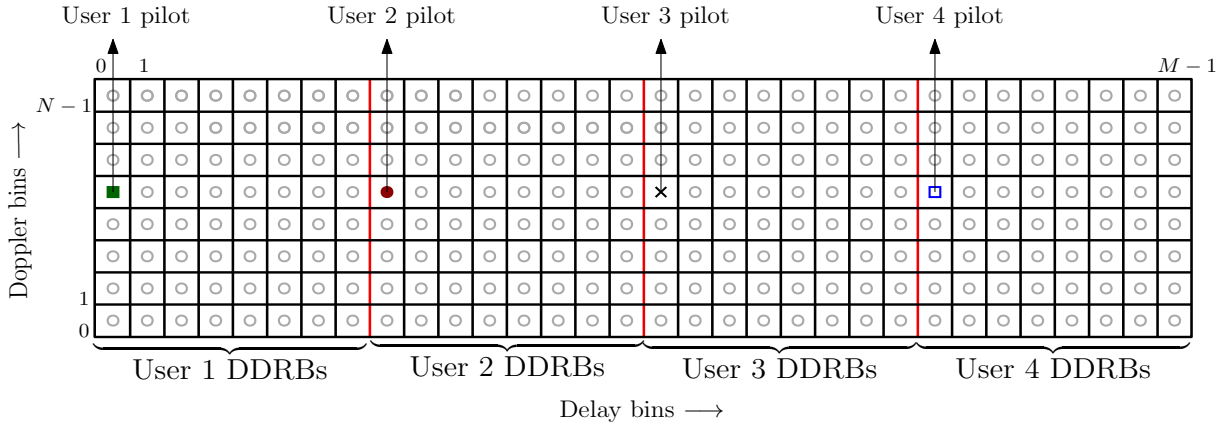


Fig. 10: Multiuser pilot placement on $N \times M$ delay-Doppler grid for Scheme 1 ('o' indicates zeros).

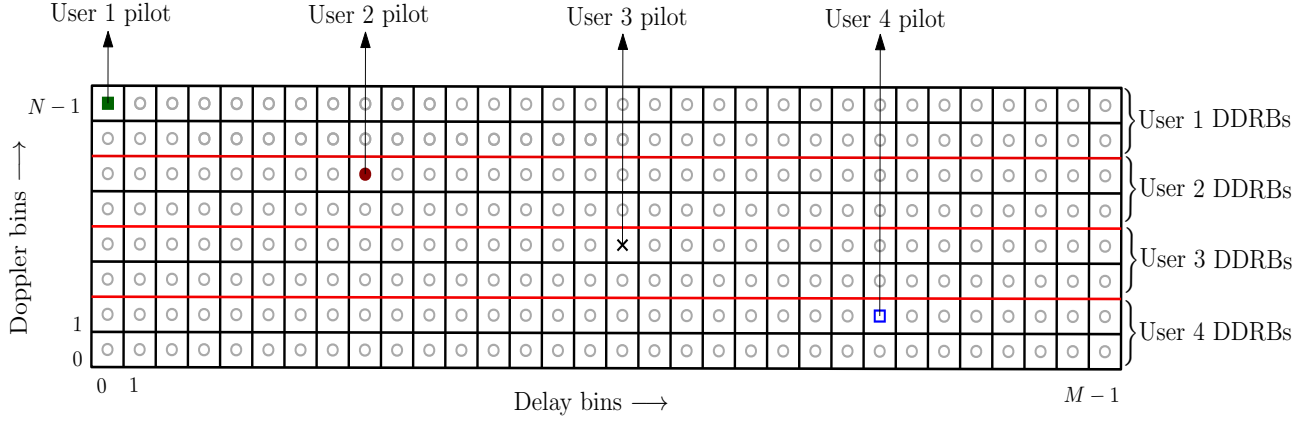


Fig. 11: Multiuser pilot placement on $N \times M$ delay-Doppler grid for Scheme 2 ('o' indicates zeros).

where (k_u^p, l_u^p) is a DDRB allocated to the u th user and $l_{u+1}^p - l_u^p > \max_i(\alpha_{u,i})$ for every u . Note that this requires $M/K_u > \max(\alpha_{u,i})$ for Scheme 1 and $M > \sum_u \max(\alpha_{u,i})$ for Scheme 2. The interaction of pilot with the channel results in a 2D convolution of the delay-Doppler impulse response with the pilot. The received pilot corresponding to the u th user can be written using (8) as

$$y_u^p[k', l'] = \frac{1}{MN} \tilde{h}_u[(k' - k_u^p)_N, (l' - l_u^p)_M] + v[k', l'], \quad (28)$$

which gives the estimated channel gains of the u th user, where $k' \in \{0, 1, \dots, N-1\}$ and $l' \in \{l_u^p, \dots, l_u^p + \max_i \alpha_{u,i}\}$. Figures 10 and 11 illustrate one of the possible ways of placing the pilots on the $N \times M = 8 \times 32$ delay-Doppler grid allocated to $K_u = 4$ users for Schemes 1 and 2, respectively, taking $\max_{u,i} \alpha_{u,i} = 7$.

A. Performance results

Figure 12 shows the normalized mean squared error (MSE) of the estimated channel as a function of pilot SNR for four users ($K_u = 4$) in uplink OTFS-MA with Scheme 1 of DDRB allocation. The channel corresponding to each user is assumed to have ten taps ($P_u = 10, \forall u$) with an exponential power delay profile and Jakes Doppler spectrum. All the other

channel parameters are same as considered for Fig. 8. The pilots are placed on $N \times M = 16 \times 64$ delay-Doppler grid for the channel estimation. From Fig. 12, we see that the normalized MSE decreases with the increase in pilot SNR and the MSE is less than 0.01 for pilot SNR larger than 36 dB. In Fig. 13, we plot the BER performance of OTFS-MA with Scheme 1 allocation with $K_u = 4$ using the channel estimation scheme described above and MP detection for different values of pilot SNR. The channel is estimated during the pilot frame which is used for detection in the subsequent data frame. From Fig. 13, it can be observed that the BER performance achieved with the estimated channel is close to the performance with perfect channel knowledge for pilot SNRs of 40 and 50 dB.

VI. CONCLUSIONS

We considered the problem of multiple access using the recently proposed OTFS modulation for multiuser communication on the uplink. Three different schemes to allocate delay-Doppler resource blocks to the users were considered. The BER performance of OTFS-MA in comparison with those of OFDMA and SC-FDMA was investigated considering ML detection for small dimension systems and message passing detection for large dimension systems. OTFS-MA was found to achieve better performance compared to OFDMA and SC-

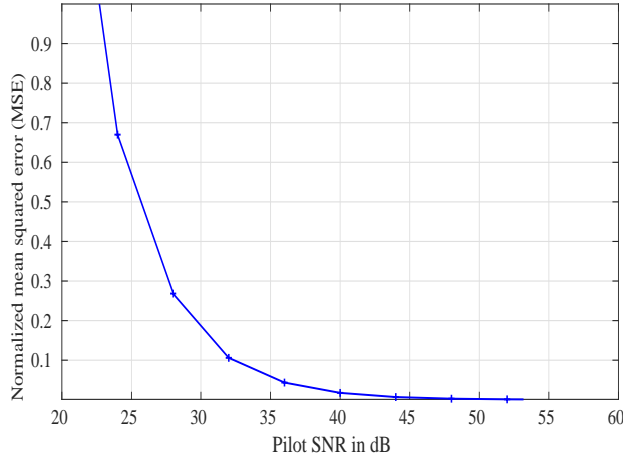


Fig. 12: Normalized mean squared error of the estimated channel in uplink OTFS-MA.

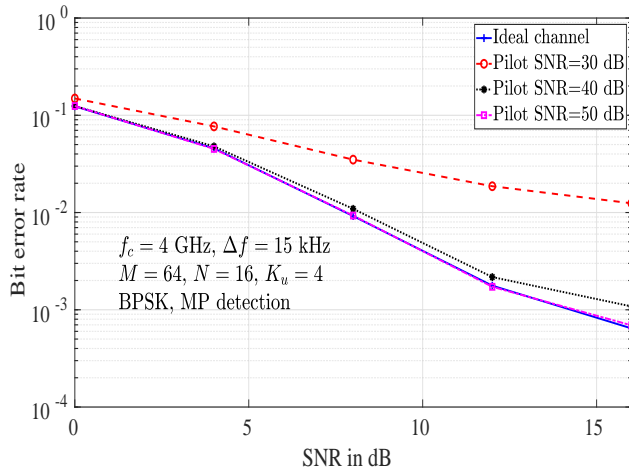


Fig. 13: BER performance of OTFS-MA with estimated channel in uplink OTFS-MA.

FDMA on the uplink in high mobility environments. Also, a pilot based channel estimation scheme in the delay-Doppler domain for OTFS-MA was shown to achieve a performance close to that with perfect channel knowledge.

REFERENCES

- [1] W. C. Jakes, *Microwave Mobile Communications*, New York: IEEE Press, reprinted, 1994.
- [2] T. Wang, J. G. Proakis, E. Masry, and J. R. Zeidler, "Performance degradation of OFDM systems due to Doppler spreading," *IEEE Trans. Wireless Commun.*, vol. 5, no. 6, pp. 1422-1432, Jun. 2006.
- [3] R. Hadani, S. Rakib, M. Tsatsanis, A. Monk, A. J. Goldsmith, A. F. Molisch, and R. Calderbank, "Orthogonal time frequency space modulation," *Proc. IEEE WCNC'2017*, pp. 1-7, Mar. 2017.
- [4] R. Hadani, S. Rakib, S. Kons, M. Tsatsanis, A. Monk, C. Ibars, J. Delfeld, Y. Hebron, A. J. Goldsmith, A. F. Molisch, and R. Calderbank, "Orthogonal time frequency space modulation," online: arXiv:1808.00519v1 [cs.IT] 1 Aug 2018.
- [5] R. Hadani and A. Monk, "OTFS: A new generation of modulation addressing the challenges of 5G," online: arXiv:1802.02623 [cs.IT] 7 Feb 2018.
- [6] R. Hadani, S. Rakib, A. F. Molisch, C. Ibars, A. Monk, M. Tsatsanis, J. Delfeld, A. Goldsmith, and R. Calderbank, "Orthogonal time frequency space (OTFS) modulation for millimeter-wave communications systems," *Proc. IEEE MTT-S Intl. Microwave Symp.*, pp. 681-683, Jun. 2017.
- [7] L. Li, H. Wei, Y. Huang, Y. Yao, W. Ling, G. Chen, P. Li, and Y. Cai, "A simple two-stage equalizer with simplified orthogonal time frequency space modulation over rapidly time-varying channels," online: arXiv:1709.02505v1 [cs.IT] 8 Sep 2017.
- [8] A. Farhang, A. R. Reyhani, L. E. Doyle, and B. Farhang-Boroujeny, "Low complexity modem structure for OFDM-based orthogonal time frequency space modulation," *IEEE Wireless Commun. Lett.*, doi: 10.1109/LWC.2017.2776942, Nov. 2017.
- [9] P. Raviteja, K. T. Phan, Y. Hong, and E. Viterbo, "Interference cancellation and iterative detection for orthogonal time frequency space modulation," *IEEE Trans. Wireless Commun.*, vol. 17, no. 10, pp. 6501-6515, Aug. 2018.
- [10] K. R. Murali and A. Chockalingam, "On OTFS modulation for high-Doppler fading channels," *Proc. ITA'2018*, San Diego, Feb. 2018.
- [11] M. K. Ramachandran and A. Chockalingam, "MIMO-OTFS in high-Doppler fading channels: signal detection and channel estimation," *Proc. IEEE GLOBECOM'2018*, Dec. 2018. Online: arXiv:1805.02209v1 [cs.IT] 6 May 2018.
- [12] G. D. Surabhi, R. M. Augustine, and A. Chockalingam, "On the diversity of OTFS modulation in doubly-dispersive channels," online: arXiv:1808.07747 [cs.IT] 23 Aug 2018.
- [13] R. M. Augustine, G. D. Surabhi, and A. Chockalingam, "Space-time coded OTFS modulation in high-Doppler channels," accepted in *IEEE VTC2019-Spring* Apr. 2019.
- [14] P. Raviteja, Y. Hong, E. Viterbo, and E. Biglieri, "Practical pulse shaping waveforms for reduced-cyclic-prefix OTFS," accepted in *IEEE Trans. Veh. Tech.* doi: 10.1109/TVT.2018.2878891.
- [15] A. Nimr, M. Chafii, M. Matthe, and G. Fettweis, "Extended GFDM framework: OTFS and GFDM comparison," online: arXiv:1808.01161v1 [eess.SP] 3 Aug 2018.
- [16] V. Khammammetti and S. K. Mohammed, "OTFS based multiple-access in high Doppler and delay spread wireless channels," accepted in *IEEE Trans. Wireless Commun.* doi: 10.1109/LWC.2018.2878740.
- [17] P. Raviteja, K. T. Phan, and Y. Hong, "Embedded Pilot-Aided Channel Estimation for OTFS in Delay-Doppler Channels," Online: arXiv:1808.08360 [cs.IT] 25 Aug 2018.
- [18] S. Rakib and R. Hadani, "Multiple access in wireless telecommunications system for high-mobility applications," *US Patent No. US9722741B1*, Aug. 2017.
- [19] D. Tse and P. Viswanath, *Fundamentals of Wireless Communication*, Cambridge University Press, 2005.
- [20] F. Hlawatsch and G. Mats, *Wireless Communications over Rapidly Time-Varying Channels*, Academic Press, 2011.